

# Noncontact single-pulse optical method to measure interfacial properties in intact systems

David C. Clark and Myung K. Kim\*

Department of Physics, University of South Florida, 4202 E. Fowler Avenue, Tampa, Florida 33620, USA

\*Corresponding author: mkkim@usf.edu

Received August 13, 2012; revised November 6, 2012; accepted November 12, 2012;  
posted November 12, 2012 (Doc. ID 173727); published December 10, 2012

We introduce a noncontact purely optical approach to measuring the localized surface properties of an interface within a system using a single optical pressure pulse and a time-resolved digital holographic quantitative phase-imaging technique to track the propagating nanometric capillary disturbance. We demonstrate the proposed method's ability to measure the surface energy of deionized water, methanol, and chemical monolayers formed by surfactants with good agreement to published values. The development of this technique boasts immediate application to static and dynamic systems and near-future applications for living biological cell membranes. © 2012 Optical Society of America

OCIS codes: 280.4788, 090.1995, 350.4855.

Interfacial analysis is a valuable tool in areas of soft-matter physics, chemistry, and biology. In fact, many surface-energy measurement techniques have been employed for their varying degrees of improvement in accuracy, precision, or adaptability. Most of these tend to be invasive to the interface and suffer from an inability to make measurements without disturbing the system. Droplet methods require a small sample to be removed from the system and tested separately [1], while probing methods require a full-contact probe through or on the interface of interest [2]. Continuous wave (cw) optical manipulation techniques, including trapping and radiation pressure, have grown popular for their noncontact nature and precise control [3,4]. Optical trapping methods, however, require a tightly focused beam, which may have unwanted effects on the media and often use microspheres as probes in contact with the interface. The loosely focused cw optical pressure techniques overcome some of these drawbacks; however, observation of the resulting weak deformation effect may be limited to very low surface tension applications, such as phase-separating microemulsions [5], and imaging that relies on surface lensing or phase modulation, both of which are also affected by imminent thermal effects, as has been shown even for very transparent media applications [6–8].

A frequency-regulated optical pressure approach that induces capillary waves on the surface of interest has been shown to provide a good measure of surface tension [9]. The method makes use of a characteristic frequency that is related to the surface tension of the interface. This frequency scanning, however, requires sustained excitation of the sample and, as mentioned in [9], is limited by thermal effects.

The approach that we introduce here makes use of the dependence of the capillary wave velocity on the surface energy of the interface. We induce a capillary wave with a single laser pulse and the propagating wavefront of only a few nanometers in amplitude is easily tracked by our time-resolved digital holographic quantitative phase microscopy (DH-QPM) imaging apparatus (Fig. 1). Due to the axisymmetry of the disturbance, we are able to use an azimuthal averaging algorithm to improve image

and tracking precision [8]. The short (5 ns) single pulse does not produce a measurable thermal signal compared to the physical deformation signal [10,11].

The initial deformation is a direct result of the conservation of photon momentum as the photon encounters a boundary of differing refractive indices [12–14]. By solving for the simple case of a flat interface with normal incident photons ( $z$ -direction) on transparent media, we have for the momentum exchange

$$\vec{p} = \frac{h\nu}{c} 2n_1 \left( \frac{n_1 - n_2}{n_1 + n_2} \right) \hat{z}, \quad (1)$$

where  $n_1$  and  $n_2$  are the refractive indices of the first and second media, respectively, and  $h\nu/c$  is the photon's momentum in vacuum. It is easy to see from this relation that the direction of momentum transfer, and therefore the initial deformation of the interface, will always point in the direction of the smaller refractive index regardless of the direction of beam propagation. The resulting phase shift will, therefore, always be positive (longer optical path length), which is opposite that of the thermal lensing effect, making the two easily distinguishable by DH-QPM [10]; however, the current method of pulsed excitation eliminates this necessity [11].

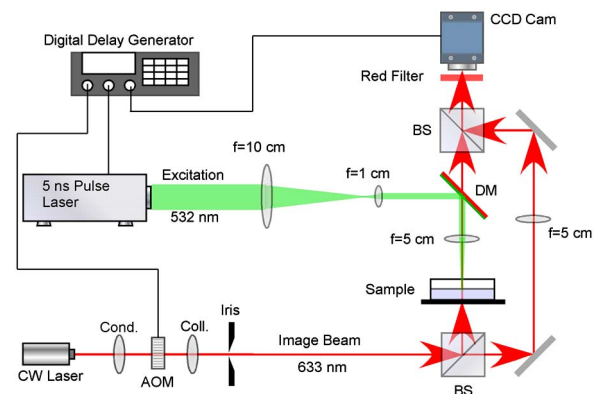


Fig. 1. (Color online) Experimental apparatus. 633 nm, imaging; 532 nm, excitation; AOM, acousto-optic modulator; BS, beam splitter; DM, dichroic mirror.

In our experiments, we track the single-pulse capillary wavefront position as a function of time to determine a surface-wave velocity. By substituting the phase velocity,  $v = \omega/\kappa$ , into the dispersion relation for capillary waves [15], we can write succinctly

$$v = \sqrt{\frac{\sigma\kappa}{\rho}}, \quad (2)$$

where  $\rho$  is the density of the liquid (that of air is justly ignored here),  $\kappa$  is the angular wavenumber, and  $\sigma$  represents the surface tension at the air–liquid interface.

We acknowledge at this point that the determination of a wavenumber is not straightforward for a single propagating pulse. A propagating pulse is a superposition of sinusoidal waves where the maximum wavenumber is the fastest and sets the wavefront velocity. For a Gaussian-like pulse, it is intuitive and reasonable to assume this wavenumber is  $2\pi$  times the inverse of the input spatial pulsewidth. Therefore, we determine our disturbance wavenumber when the source deformation reaches its maximum height. At this time step, the half wavelength, and therefore the wavenumber, can be determined by the horizontal distance from the center to the minima of the deformation. This method of determining our single-pulse wavenumber has been sustained empirically by control experiments. We shift  $t = 0$  to this time step and, by integrating Eq. (2) with respect to time, we can write the linear expression for position,

$$r(t) = t\sqrt{\frac{\sigma\kappa}{\rho}} + r_0, \quad (3)$$

where  $r_0 = \pi/\kappa$  as defined above by our initial boundary condition. We note here that it is only necessary to create an observable capillary disturbance and is not necessary to have additional knowledge of properties and parameters that may describe the deformation itself.

The diagram of the experimental apparatus is shown in Fig. 1 and is similar to that developed in our previous work [11]. A Mach–Zehnder interferometer is used to create the hologram of the sample using low power (<1 mW) 633 nm laser light. The reference and object beams each follow a similar path, through matching objective lenses, before recombining by a beam splitter. The interference of the phase-modulated object beam with the reference beam creates the hologram and is recorded by a digital CCD camera placed atop the setup. The holograms are processed by our LabVIEW personal computer platform for amplitude and phase reconstruction based on the angular spectrum method [16].

An integrated optical excitation arm delivers a 532 nm, 5 ns pulse to the system. The pulse energy is adjustable from 0–25 mJ with a built-in attenuator. For all present experiments, the output was set to  $\sim 5$  mJ. The pulse beam is passed through a 10:1 focal length lens pair to create a much reduced beam radius. A dichroic mirror reflects this excitation beam down toward the sample while allowing the probe beam to transmit up toward the CCD camera. The excitation beam passes through the shared objective lens, which loosely focuses the already narrowed beam through the sample area. The

objectives are chosen to have long effective focal lengths to aid in maintaining constant beam radius at the interface ( $\sim 100$   $\mu\text{m}$  presently). A removable red bandpass filter is placed just in front of the CCD camera to filter out any excitation light leaking through the dichroic mirror.

The sample consists of a partially liquid-filled modified glass cuvette 10 by 40 by 45 mm with a sealable lid. The cuvette is placed on the sample stage on its side oriented with a 10 mm path length. The liquid level in the cuvette is filled to a height of 5 mm in this orientation. The modified cuvette has a small ( $\sim 6$  mm) hole drilled through the upper glass surface providing an unimpeded excitation beam delivery. All general phase aberration, including wavefront curvature mismatch, can be easily compensated for by storing a background phase image prior to excitation and subtracting this from the excited images. Additional compensation for the inherent dynamic nature of the free liquid surface is also easily achieved as needed with DH-QPM.

A digital delay generator (DDG) with picosecond-resolution capability controls precise timing of both excitation and imaging. Prior to delivery to the system, the imaging beam is condensed through an acousto-optic modulator (AOM), which, during triggering, diffracts the imaging beam through a collimating lens and iris into the system. The DDG signals the camera to remain open while sending a 5  $\mu\text{s}$  square pulse signal to this AOM shutter system at specified delay times after the excitation pulse. This delivery method produces the short exposure images required for this study without sacrificing phase quality. Note that all additional hardware delays were measured independently by oscilloscope study and compensated for by the DDG.

We have employed here a time-resolved imaging technique that requires each time step to be the result of a separate optical pressure pulse followed by an appropriately delayed short (5  $\mu\text{s}$ ) camera exposure. This introduces some uncertainty due to variation in the output energy of each pulse. The use of a high-speed camera or alternative rapid imaging method may eliminate this uncertainty; however, the demonstration of our proposed technique's capabilities is affected little by this. Several resulting time-sensitive phase images and corresponding treated three-dimensional (3D) reconstructions are displayed in Fig. 2. The capillary wavefront is visible as the expanding minima ring. From Eq. (3) and the position of this minima in time, the slope of the linear fits (least-squares method) to example time-series data in Fig. 3

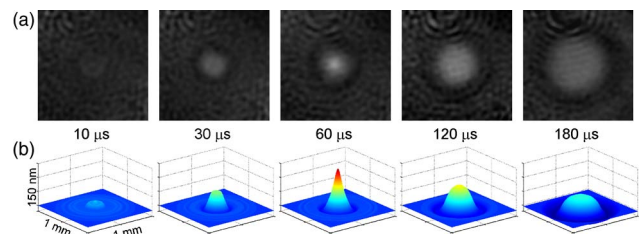


Fig. 2. (Color online) Time-dependent surface response to optical impulse for DI water. (a) Raw phase images ( $1.0 \times 1.0$  mm) of selected time steps and (b) corresponding azimuthal averaged 3D reconstruction ( $1.0 \text{ mm} \times 1.0 \text{ mm} \times 150 \text{ nm}$ ).

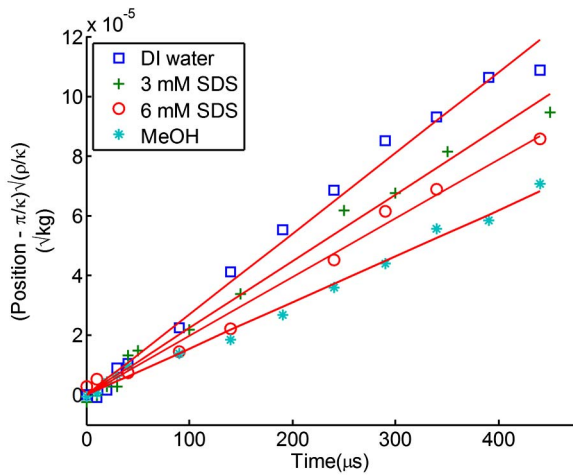


Fig. 3. (Color online) Comparison of  $(r(t) - r_0)\sqrt{(\rho/\kappa)}$  versus  $t$  for each sample, where the square of each slope is equal to the surface tension.

reveals the surface energy measurements discussed below. Note that, as described earlier, a single wavenumber is determined for each series leaving no free parameters in this fitting.

First, we characterized our technique for known substances at both high and low surface energy standards. For the high range, we chose the deionized (DI) water–air interface, as the expected value is well known to be 72.8 mN/m [17]. Our measured value was  $72.9 \pm 0.6$  mN/m where the tolerance here represents the standard deviation of repeated trials. For the low-range standard, we chose the methanol–air interface with a previously reported surface energy of 22.6–22.9 mN/m [17,18] and we have measured this to be  $23.8 \pm 0.3$  mN/m.

Some differences in these values may be expected due to the noncontact nature of our approach versus the traditional probe. Here, we assume that the above measurements are reasonably close to expected values and continue with the application of our method to chemical monolayers. Again, we have chosen a well-known surfactant, sodium dodecyl sulfate (SDS), whose effect on the water–air interface has been studied previously [19].

We measured the surface energy at the solution–air interfaces of 3 and 6 mM SDS concentrations in DI water. Our results of 50.1 and 38.9 mN/m, respectively, are within the expected range for typical stock solutions at these concentrations [19]. Variations around measured values for such mixtures are discussed at length in the cited reference. It is beyond the scope of our study to address this; however, the dynamic nature of monolayers presents a favorable application for our method. While surface tension is traditionally treated as a characteristic property of an entire interface, the surface energy may likely vary from region to region based on localized conditions, particularly in this case. The technique we have presented is adapted to this kind of localized measurement, which may often be important.

There are several advantages inherent to the method described here. Since the excitation requires only a refractive-index difference and the imaging is QPM, a broad selection of laser sources will perform the tasks with little or no consequence. DH-QPM has been shown to

measure optical path differences of less than 1 nm [8], making it well suited for observation of very small physical disturbances qualifying the use of mild excitation pulses. Also, it is easy to numerically propagate to different planes of focus within a single time series of holograms if desired [20]. Furthermore, the method is well suited for low surface energy applications since the capillary wavefront velocity will be reduced and the deformation will occur with less applied pressure.

We have demonstrated a noncontact, noninvasive, purely optical approach to accurately measure the surface tension of highly transparent pure substances and chemical monolayers. More absorptive applications may still generate thermal issues, which may be avoided by choice of excitation wavelength or use of reflection instead of transmission. In fact, we believe the method can be extended to the study of biological membranes, which has long been a topic of interest [21,22]. Of particular need are optical techniques that can perform this analysis in living cells as they undergo natural processes and life-cycle behavior without excessive stretching or contact probes [23,24].

## References

1. S.-Y. Lin and H.-F. Hwang, *Langmuir* **10**, 4703 (1994).
2. E. I. Franses, O. A. Basaran, and C.-H. Chang, *Curr. Opin. Colloid Interface Sci.* **1**, 296 (1996).
3. A. Ashkin, *IEEE J. Sel. Top. Quantum Electron.* **6**, 841 (2000).
4. K. Sakai, D. Mizuno, and K. Takagi, *Phys. Rev. E* **63**, 046302 (2001).
5. A. Casner and J.-P. Delville, *Opt. Lett.* **26**, 1418 (2001).
6. A. Marcano, C. Loper, and N. Melikechi, *Appl. Phys. Lett.* **78**, 3415 (2001).
7. D. C. Clark and M. K. Kim, *Appl. Opt.* **50**, 1668 (2011).
8. D. C. Clark and M. K. Kim, *Chin. Opt. Lett.* **9**, 120001 (2011).
9. S. Mitani and K. Sakai, *Phys. Rev. E* **66**, 031604 (2002).
10. D. C. Clark and M. K. Kim, in *Frontiers in Optics*, OSA Technical Digest (Optical Society of America, 2011), paper FThU5.
11. D. C. Clark and M. K. Kim, in *Digital Holography and Three-Dimensional Imaging*, OSA Technical Digest (Optical Society of America, 2012), paper DW1C.5.
12. A. Ashkin and J. M. Dziedzic, *Phys. Rev. Lett.* **30**, 139 (1973).
13. I. I. Komissarova, G. V. Ostrovskaya, and E. N. Shedova, *Opt. Commun.* **66**, 15 (1988).
14. B. Issenmann, R. Wunenburger, H. Chraïbi, M. Gandil, and J.-P. Delville, *J. Fluid Mech.* **682**, 460 (2011).
15. L. D. Landau and E. M. Lifshitz, *Fluid Mechanics* (Pergamon, 1959).
16. M. K. Kim, *SPIE Rev.* **1**, 018005 (2010).
17. G. Vazquez, E. Alvarez, and J. M. Navaza, *J. Chem. Eng. Data* **40**, 611 (1995).
18. M. Součková, J. Klomfar, and J. Pátek, *J. Chem. Eng. Data* **53**, 2233 (2008).
19. K. J. Mysels, *Langmuir* **2**, 423 (1986).
20. M. Kim, *Digital Holographic Microscopy: Principles, Techniques, and Applications* (Springer, 2011).
21. J. Spelt, D. Absolom, W. Zingg, C. van Oss, and A. Neumann, *Cell Biophys.* **4**, 117 (1982).
22. R. David, H. Ninomiya, R. Winklbauer, and A. W. Neumann, *Colloids Surf. B* **72**, 236 (2009).
23. J. Guck, R. Ananthakrishnan, H. Mahmood, T. J. Moon, C. C. Cunningham, and J. Käs, *Biophys. J.* **81**, 767 (2001).
24. J. Dai and M. P. Sheetz, *Biophys. J.* **68**, 988 (1995).